International Tables for Crystallography (2006). Vol. C, Section 2.9.5, pp. 128–129.

2.9.4. Surface roughness

Up to this point, we have only considered reflection from smooth, flat surfaces. In reality, however, all surfaces have microscopic or mesoscopic imperfections such as steps, facets and rough hills and valleys. In this case, the potential must be represented by a three-dimensional function instead of the simple one-dimensional example discussed above. In addition, the roughness may not be confined to the outer surface or substrate, but the imperfections may propagate through several layers. This roughness at the interfaces modifies the specularly reflected beam and adds a diffuse component to the scattered beam (*i.e.* neutrons scattered at angles other than the incident angle). Theories based on the distorted-wave, Born approximation have been developed to describe this type of scattering (Nevot & Croce, 1980; Sinha, Sirota, Garroff & Stanley, 1988; Pynn, 1992; Sears, 1993; Holy, Kubena, Ohlidal, Lischka & Plotz, 1993; de Boer, 1994) for a microscopically rough surface. These theories give results consistent with the earlier work (Nevot & Croce, 1980) for the modification to the specular scattering due to a single rough surface. The reader is referred to Sinha, Sirota, Garroff & Stanley (1988) and Pynn (1992) for a more complete discussion of diffuse scattering.

In order to fit the specular scattering from a rough surface, two simple methods have been employed. First, using the matrix method discussed above, the rough interface can be modelled as a smoothly varying scattering density approximated as a series of steps. This has the advantage that complex interfaces that are combinations of rough surfaces and intermixed layers can be approximated. The other method is to extend the results of Nevot to each successive interface while iteratively calculating the reflection amplitude. This method works well for simple interfaces of Gaussian roughness and is faster, in general, than the matrix method, since fewer calculations are needed for each interface. However, this latter technique suffers from frequently yielding unphysical answers (*i.e.* surface widths greater than adjacent layer thicknesses). Both of these methods are inadequate, in that there is no way to separate the effects of graded interfaces from rough surfaces. This can only be done with a simultaneous examination of both the diffuse and specular scattering.

2.9.5. Experimental methodology

Neutron reflectivity measurements can be carried out in two principal ways: either (1) with a monochromatic incident beam of narrow angular divergence in the plane of reflection (defined by $\mathbf{k}_i$ and $\mathbf{k}_f$, where λ is constant, and Q is varied by changing the glancing angle of incidence, θ, relative to the sample surface; or (2) using a pulsed polychromatic incident beam, also of narrow angular divergence at fixed θ, and obtaining data over a range of Q values simultaneously by performing time-of-flight analysis on the reflected neutrons. For either method, the instrumental resolution is simply given as

$$\left(\frac{\Delta Q}{Q}\right)^2 = \left(\frac{\Delta\lambda}{\lambda}\right)^2 + \left(\frac{\Delta\theta}{\theta}\right)^2, \qquad (2.9.5.1)$$

where $\Delta\theta$ is the angular divergence of the reflected beam, and $\Delta\lambda$ is the wavelength spread. In the case of a steady-state source,

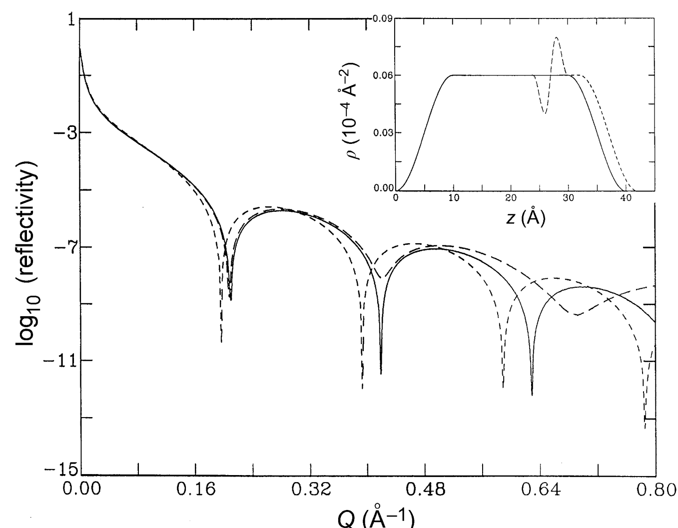

Fig. 2.9.6.1. Calculated neutron reflectivity curves corresponding to the three density profiles in the inset (*i.e.* solid line in density profile corresponds to solid line in reflectivity plot). Note that in the density plots the solid and long-dash curves coincide except at the oscillation on top of the plateau, whereas the solid and short-dashed curves coincide except at the trailing edge between 30 and 42 Å.

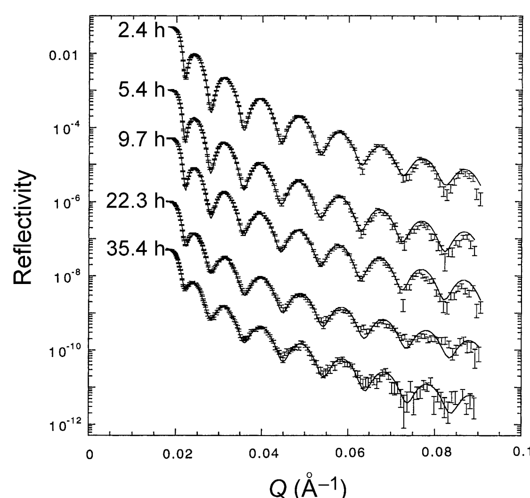

Fig. 2.9.7.1. Measured neutron reflectivities from boron bilayers [from Smith *et al.* (1992)].

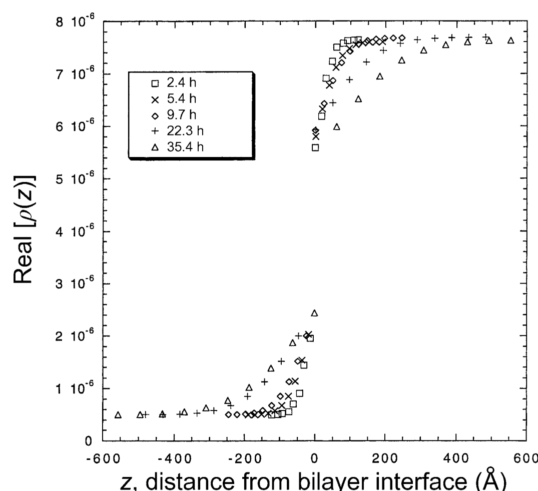

Fig. 2.9.7.2. The fitted real part of the scattering density profiles for the measured reflectivities of Fig. 2.9.7.1. Note the pinning of the concentration of ^{10}B at the interface [after Smith *et al.* (1992)].

Copyright © 2006 International Union of Crystallography

the wavelength resolution is determined by the monochromator, whereas the timing and moderator characteristics determine the wavelength resolution on a time-of-flight instrument. Although the second term in equation (2.9.5.1) is standard in scattering, it has a unique characteristic, in that the angular divergence of the reflected beam determines the resolution. This is the case because the sample is a δ-function scatterer, so that the angle of the incident beam can be determined precisely by knowing the reflected angle (Hamilton, Hayter & Smith, 1994). For a more complete description of both types of neutron reflectometry instrumentation, see Russell (1990).

2.9.6. Resolution in real space

From Fig. 2.9.2.3, the period δQ of the reflectivity oscillation (in the region where the Born approximation becomes valid, sufficiently far away from the critical angle) is inversely proportional to the thickness t of the film. That is, $2\pi/(\delta Q) = t$. Consequently, in order to be able to resolve reflectivity oscillations for a film of thickness t, the instrumental Q resolution ΔQ [from equation (2.9.5.1)] must be approximately $2\pi/t$ or smaller. With sufficiently good instrumental resolution, even the thickness of a film with non-abrupt interfaces can be accurately determined, as demonstrated by the hypothetical case depicted in Fig. 2.9.6.1 (where the instrumental resolution is taken to be perfect): an overall film-thickness difference of 2 Å (between 42 and 40 Å films) is clearly resolved at a Q of about 0.2 Å^{-1}. In practice, differences even less than this can be distinguished. Note, however, that to 'see' more detailed features in the scattering-density profile (such as the oscillation on top of the plateau shown for the long-dash profile in the inset of Fig. 2.9.6.1), other than the overall film thickness, it can be necessary to make reflectivity measurements at values of Q corresponding to 2π/(characteristic dimension of the feature).

2.9.7. Applications of neutron reflectometry

2.9.7.1. *Self-diffusion*

One of the simplest, yet powerful, examples of the use of neutron reflectivity is in the study of self-diffusion. Most techniques to measure diffusion coefficients rely on chemical and mechanical methods to measure density profiles after a sample

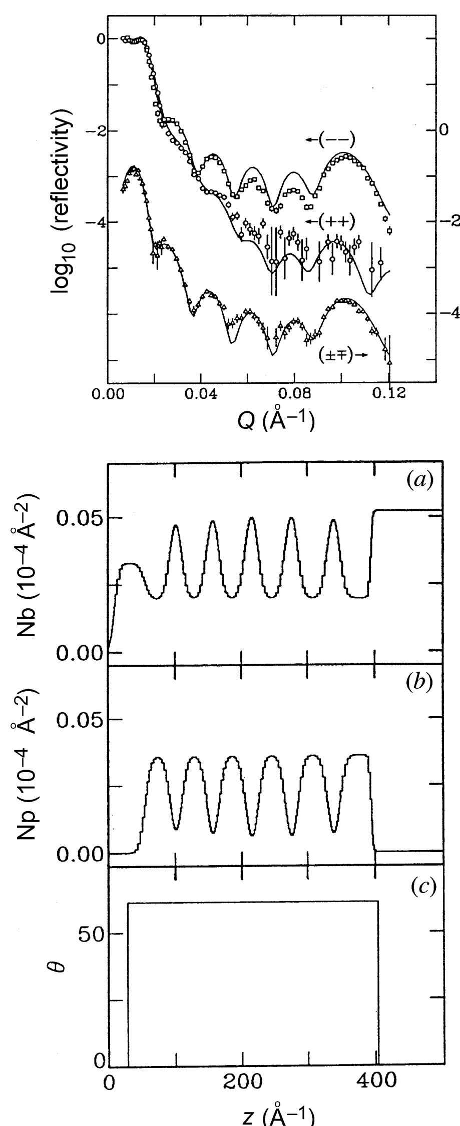

Fig. 2.9.7.3. Co/Cu(111) spin-dependent reflectivities (top). Nuclear (Nb) and magnetic (Np) scattering densities (bottom). Also shown is the (constant) moment direction [after Schreyer *et al.* (1993)].

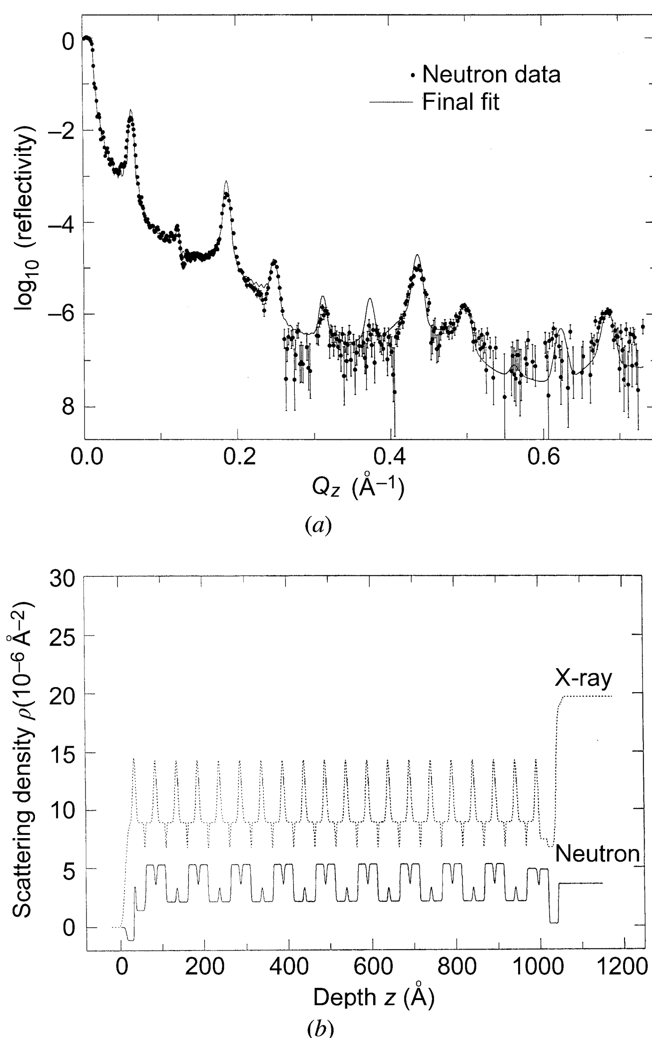

Fig. 2.9.7.4. (*a*) Measured neutron reflectivity for the Langmuir–Blodgett multilayer described in the text along with the fit. (*b*) Both corresponding neutron and X-ray scattering density profiles. The X-ray reflectivity is more sensitive to the high-Z barium in the head groups whereas the neutron reflectivity can distinguish mixing between adjacent hydrogenated and deuterated hydrocarbon tails [after Wiesler *et al.* (1995)].

references